



ISSN: 0067-2904

## Synthesis and Characterization of Aluminum Doped Zinc Oxide Nanostructures by Nd:YAG Laser in Liquid

Khawla S. Khashan\*, Ghassan M. Sulaiman, Sura A. Hussain  
Department of Applied Sciences, University of Technology, Baghdad, Iraq

Received: 11/11/2019

Accepted: 30/4/2020

### Abstract

Aluminum doped zinc oxide nanoparticles (AZO) with different doping concentrations were prepared by Nd-YAG laser ablation of target in deionized water. The characterization of these nanoparticles was performed using Fourier transform infrared (FTIR) spectroscopy, scanning electron microscopy (SEM) and photoluminescence spectroscopy (PL). FTIR spectra confirmed the formation of vibrational bonds for ZnO NPs and AZO NPs. SEM images illustrated that the size and shape of the NPs changed with changing the number of laser pulses. Photoluminescence peaks exhibited two emission peaks, one at the UV region and the second in the visible region, which were modified as the number of laser pulses and doping concentration were changed.

**Keywords:** Nanostructure; Al-doped ZnO nanoparticles; Laser ablation in liquid; Nanocomposite

## تحضير وتشخيص التركيب النانوية لأكسيد الزنك المدعم بالألمنيوم بواسطة ليزر Nd: YAG في السائل

خولة صلاح خشان\* ، غسان محمد سليمان ، سري حسين

قسم العلوم التطبيقية ، الجامعة التكنولوجية ، بغداد، العراق

### الخلاصة

تم تحضير الجسيمات النانوية لأكسيد الزنك المشوبة بالألمنيوم (AZO) وبتراكيز اشابة مختلفة بواسطة الاستئصال بالليزر Nd-YAG للهدف في الماء. تم توصيف هذه الجسيمات النانوية باستخدام التحليل الطيفي بتحويل فورييه بالأشعة تحت الحمراء (FTIR) والفحص المجهر الإلكتروني (SEM) والتحليل الطيفي الضوئي (PL). اثبتت أطيايف FTIR تكوين الروابط الاهتزازية لـ ZnO NPs و AZO NPs . أوضحت صور SEM أن حجم الجسيمات النانوية NPs وشكلها يتغيران مع التغيير في عدد نبضات الليزر ، أظهرت قمم PL ذروتين للانبعاث واحدة في منطقة الأشعة فوق البنفسجية والثانية في المنطقة المرئية ، والتي تعدل حسب عدد نبضات الليزر وتغير تركيز الاشابة.

### Introduction

Pulse laser ablation in liquid (PLAL) is a media of solid target approach that is considered as an efficient technique to prepare materials in nanoscale size, due to many advantages, such as being simple, clean, and of high purity production [1]. Therefore, this process could be utilized to synthesize

\*Email: khawla\_salah@yahoo.com

different types of nanomaterials with various shapes of nanoparticles. Furthermore, it can be used to reduce the size of initial particles in liquid, by reshaping and de-agglomerating the nanoparticles [2-10]. In general, nanosize structure materials have a great importance in recent years because of their good properties and their perfect applications in different fields [11-17]. Among them, zinc oxide (ZnO) is one of the promising nanomaterials prepared in different methods, owing to the wide range of applications in optoelectronic devices, energy storage, and biomedical sciences [18-22]. In addition, the properties of this material can be enhanced by doping with different metals, such as Mg, Ti, Cd, In and Al. Therefore, we used here the two-step PLAL to prepare Al-doped ZnO nanoparticles with different concentrations and investigated their properties.

### Experimental work

Zinc metal (99.9%) was used as a solid target with dimensions of 10x10mm and a thickness of 1mm. High intense Q-switching Nd-YAG laser system at a wavelength of 1064nm was applied to irradiate the surface of the zinc target, which was impressed in small glass vessel containing 3ml of DIW. Continuous spinning was applied by a simple stirrer to avoid target agent. The height of water above the target was 2mm, while the laser beam was focused at the surface of the target by a convex lens with a focal length of 100mm. An energy at 700mJ was applied with different numbers of pulses (25, 50, 75, 100 and 125). After the preparation of ZnONPs, the zinc target was replaced by the Aluminum target (1mm thick with a purity of 99.99%) and then ablated with constant energy (700mJ) at different numbers of laser pulses (20, 30, 40 and 50), as shown in Figure-1. A microbalance scale was used to determine the mass concentration ( $M_c$ ) of the colloidal nanoparticles by weighing the bulk target before and after the nanoparticle production process. Then, the doping ratio ( $D_r\%$ ) was calculated by dividing the mass concentration of Al NPs to that of the total composition (Al+ZnO), as follows:

$$DR\% = \frac{M_c(Al)}{M_c(Al + ZnO)}$$

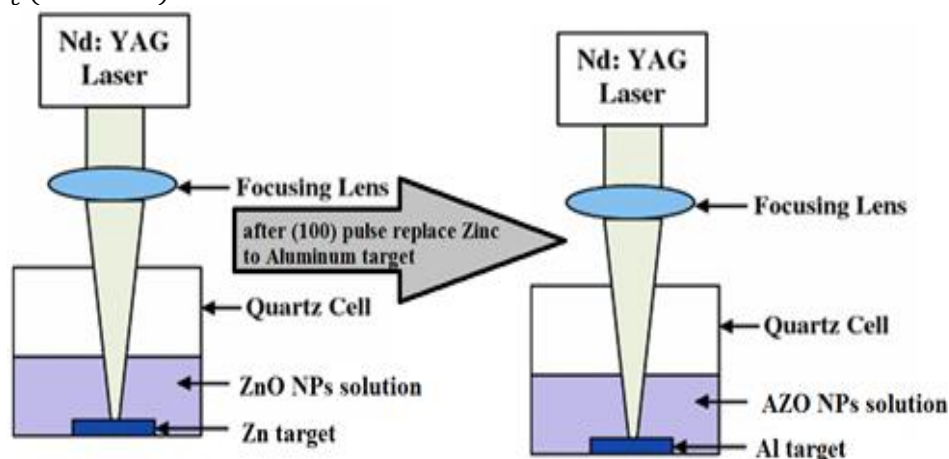


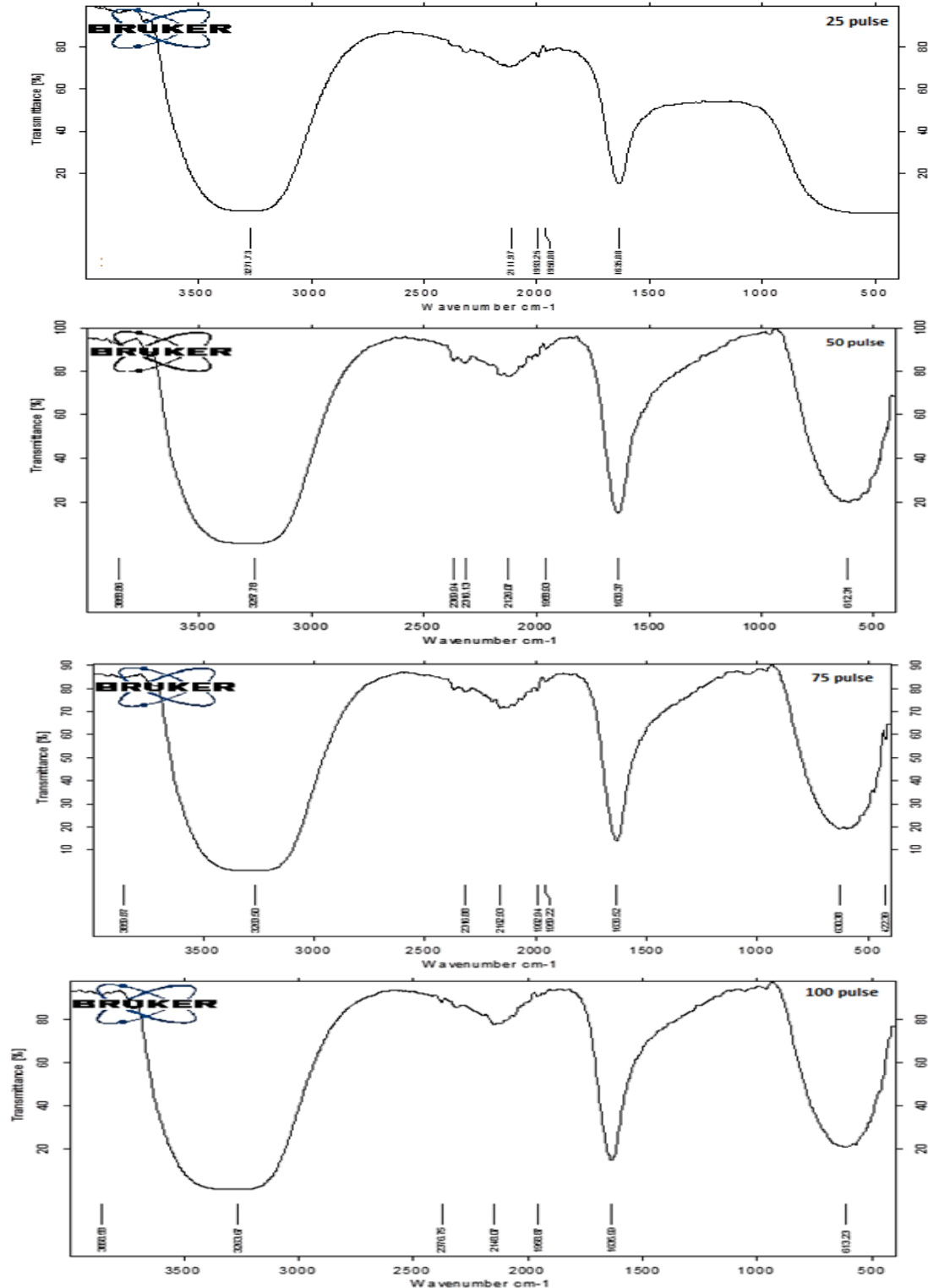
**Figure 1**-Experimental set-up for the prepared ZnO NPs and AZO NPs

The chemical bonds of the nanoparticles were studied using FTIR spectroscopy (Shimadzu, 8000 Series) with a spectral range of 500-4000  $\text{cm}^{-1}$ . For the determination of the morphological properties of the NPs, a scanning electron microscope (MERA3 TE scan) operating with 10KeV voltage was employed. The optical properties of the NP suspensions were analyzed using Shimadzu-1800 ultraviolet-visible spectrophotometer. The photoluminescence spectra of the suspensions were analyzed using a Shimadzu RF-551 photoluminescence spectroscopy system.

### Results and discussion

Figure-1 shows the FTIR spectra of ZnO nanoparticles prepared by laser ablation in liquid at different numbers of pulses (25, 50, 75, 100, and 125). In general, peaks between 410-495  $\text{cm}^{-1}$  explained the vibrational bonds for ZnO NPs, which were increased with decreasing the particles size [23]. Also, the absorption peaks at 668  $\text{cm}^{-1}$  referred to the stretching vibration of ZnO nanoparticles, and the peak at 800  $\text{cm}^{-1}$  existed due to the formation of tetrahedral coordination of zinc [24]. The peaks between 1600 -1690  $\text{cm}^{-1}$  corresponded to O-H stretching mode, the absorption peak at 2360-2390  $\text{cm}^{-1}$  corresponded to the presence of  $\text{CO}_2$  molecules in the ambient air [23], while the peak at

2900 $\text{cm}^{-1}$  corresponded to C-H stretching vibration. The absorption peaks at 3200-3600  $\text{cm}^{-1}$  correlated to the water (O-H) stretching vibration and the bending vibration [19]. Figure-2 shows the FTIR spectra of AZO nanoparticles prepared by laser ablation in DIW with different doping ratios. In general, there were the same peaks as those for Zn-O vibrations, with a new band at 615-635  $\text{cm}^{-1}$  that refers to the presence of aluminum oxide (Al-O) nanoparticles, while peaks at 1636 and 3526  $\text{cm}^{-1}$  referred to the stretching vibration of water molecules [13]. In general, increasing the number of laser pulses resulted in increased concentrations of the nanoparticles in the solution, which caused a decrease in the absorption peaks. These results are in agreement with previously published data [25,26].



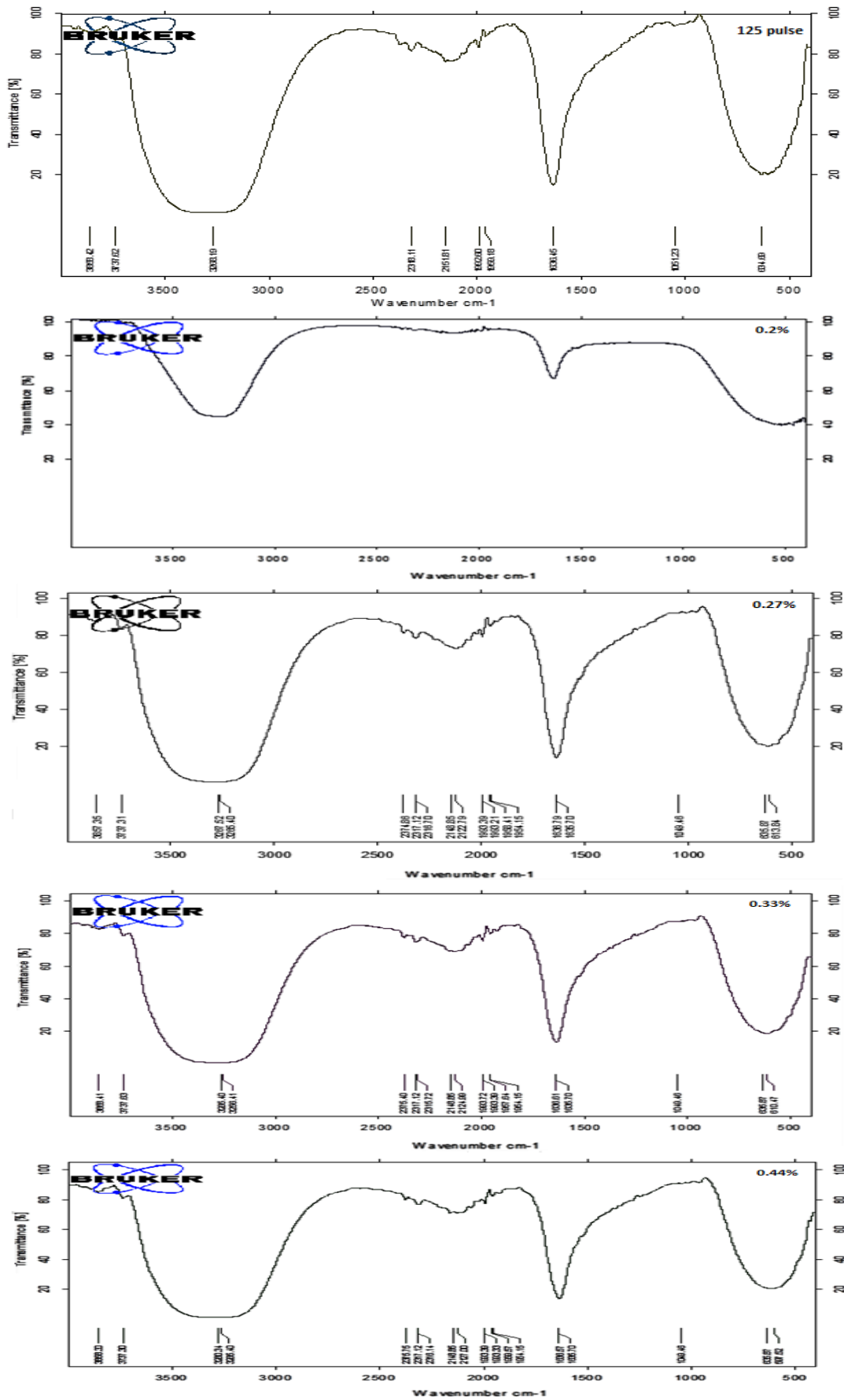
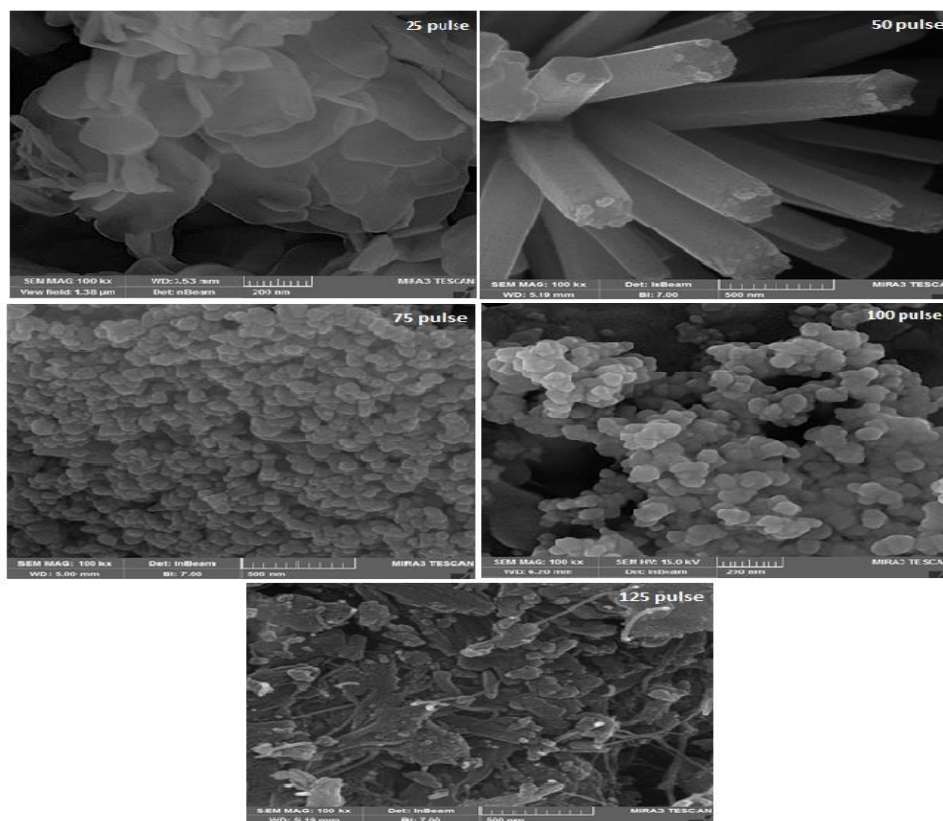


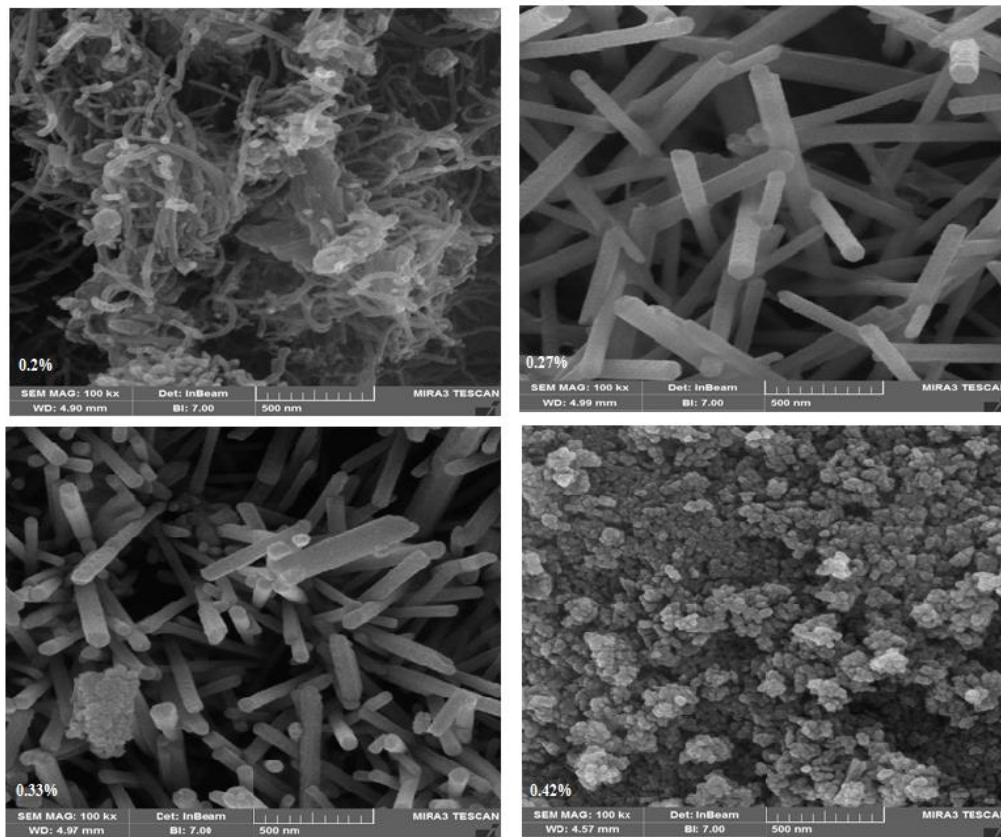
Figure 2-FTIR spectra for AZO nanoparticles prepared at different Al doping ratios

Figure-3 illustrates the SEM images for ZnO NPs synthesized by laser ablation at 700mJ as an output energy, with different numbers of pulses (25, 50, 75, 100, and 125). In general, the morphology of the prepared colloidal films was changed according to the number of laser pulses. One can observe the formation of nanoparticles which are in the shape of nan-plate or flakes with a thickness of about 10-50 nm at 25 pulses. This structure was modified to hexagonal-rod shapes at 50 laser pulses. Then, remarkable changes in the morphology were observed at 75 pulses, with the formation of spherical particles and a diameter change from 24 to 42 nm. At 100 laser pulses, an agglomerate of spherical particles along with flakes morphology could be clearly seen, but the spherical shaped morphology was mostly observed with diameter change from 34nm to 69nm. Nanowires and a tiny agglomerate of spherical nanoparticles were observed at 125 pluses. The nanowire was with a diameter of about 30nm and the particles had a diameter ranging from 22 nm to 31nm. These results are in agreement with those of previously published data [27, 28]. Figure-4 shows SEM results for Aluminum doped ZnO at different concentrations. One can notice that the morphology at 0.2% Al has a nanowire-like structure with 28nm thickness, along with some irregular particles with diameters of about 16-27 nm. At 0.27% Al, the morphology was changed to a hexagonal nanorod shape with a cross section diameter of about 126nm and a thickness of about 88-95 nm. The morphology still showed the same structure with few spherical particles as the doping ratio was increased to 0.33% Al. At this ratio, the thickness of the nanorod was decreased to 56-64 nm and the diameter of the spherical particles was 18-22 nm. Finally, the structure was modified to spherical particles with a high aggregation and a diameter of about 22-32 nm. These results are in agreement with those of earlier works [29-31]. Figure-5 explains the transmittance spectra for the prepared samples. From Figure- 5a, it is clear that the transmittance was decreased with increasing laser pulse, due to the increase in the concentration of NPs in the solution. While the transmittance was increased with Aluminum doping, as shown in Figure-5b, and it was increased as Aluminum doping ratio was increased. In general, the absorbance was low at the gap edge while the transmittance was high, which implies that the obtained samples are of low impurities and have few lattice defects. Also, the flat aspect of the transmission curve without interference fringes emphasizes the surface uniformity with small crystallite size. Due to this characteristic, these structures are used as high-performance, low-cost, optoelectronic devices [9, 13, 26].



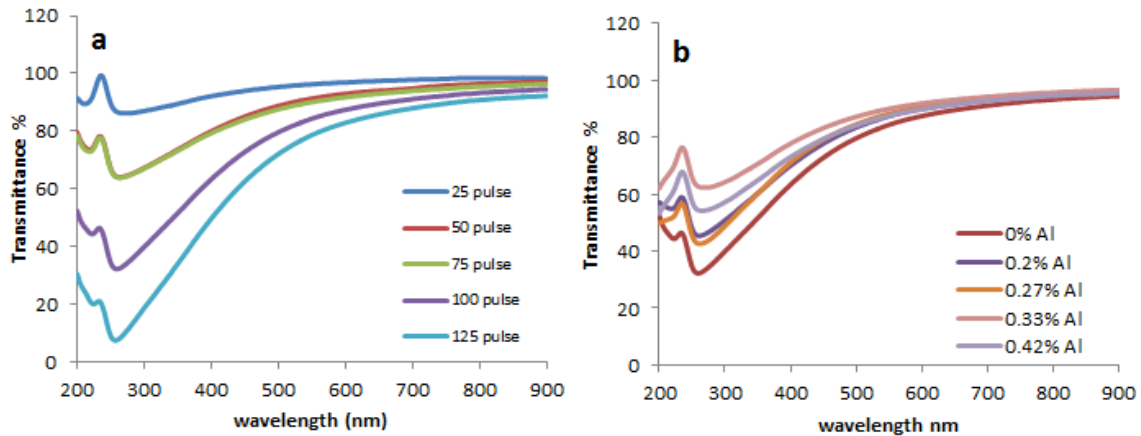
**Figure 3-**SEM image of ZnO NPs synthesized with different number of pulses

Figure-6 shows PL spectra for ZnO NPs prepared by laser ablation in liquid with different number of pulses. These samples had two emissions, one with a high intensity in the UV region at 350 nm, which is attributed to the band-edge emission or the excitation transition, and the other was with a low intensity and located in the visible region at 700 nm [19], due to the recombination of photo generated holes with singly ionized charge states which have intrinsic defects such as oxygen vacancies, Zn interstitials, or impurities. These defects caused a red-shift in the ZnO colloidal particles prepared by pulse laser ablation in liquid, which is in full agreement with the literature [20]. Increasing the number of pulses led to an increase in the number of small nanoparticles, due to the interaction between the large ZnO NPs and the high intense pulses, which led to an increase in the absorption of UV light. Thus, PL intensity was increased with increasing the number of pulses, which indicates a high concentration of ZnO NPs in the same size. Also, the sharp peaks indicated high optical properties [23, 24].



**Figure 4-**SEM images of AZO with different doping ratios

Figure-7 demonstrates the PL intensity spectra for AZO NPs prepared by laser ablation in DIW. Photoluminescence peaks exhibited two emission peaks, a strong and weak ones. The first was at the UV zone near the band edge emission centered at 350 nm. This was due to the transition from the conduction band to the valance band with PL intensity higher than the intensity of pure ZnO NPs, because of increasing aluminum concentration which substitute zinc ions in unit cell to generate the complex AZO [13]. The second band was centered at 700 nm in the visible region due to aluminum incorporation. This band was developed due to high crystallinity generated by the various  $Al^{+3}$  concentrations [32].



**Figure 5** (a)-Transmittance spectra of ZnO NPs prepared at different numbers of pulses, (b) Transmittance spectra for AZO NPs prepared at different Al doping ratios

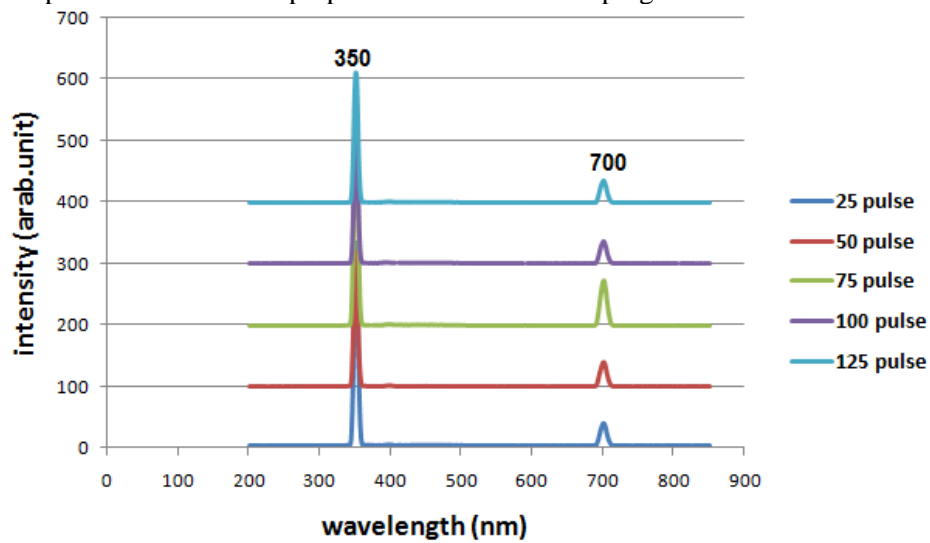


**Figure 6**-PL spectra of ZnO NPs with different numbers of pulses

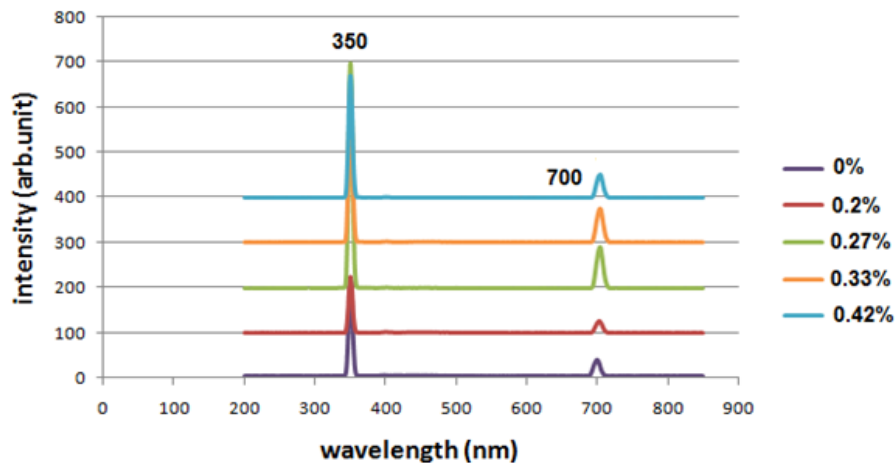


**Figure 7**-PL spectra for AZO NPs with different doping ratios

**Conclusions**

In conclusion, the method of pulse laser ablation in liquid was an efficient simple process to synthesize Al-doped ZnO NPs with different concentrations. FTIR spectra confirmed the formation of the ZnO NPs and AZO NPs. SEM images showed that ZnO NPs were changed from nano-plate to nano-wire particles with increasing the number of laser pulses, whereas they were modified from

nano-wire to spherical particles with high aggregation upon increasing the doping ratio. PL spectra were also increased as a response to the increase in the number of laser pulses and Al concentration.

## References

1. Sadrolhosseini, A. R., Mahdi, M. R., Alizadeh, F. and Abdul Rashid, S. **2018**. Laser Ablation Technique for Synthesis of Metal Nanoparticle in Liquid, *Laser Technology and its Applications*, Yufei Ma, IntechOpen, DOI: 10.5772/intechopen.80374.
2. Rao, S., Venugopal, G., Krishna, P. and Syed, H. **2014**. Ultrafast laser ablation in liquids for nanomaterials and applications. *Journal of nanoscience and nanotechnology*, **14**: 1364-1388
3. Khashan, K. S., Sulaiman, G. M. and Mahdi, M. R. **2017**. Preparation of Iron Oxide Nanoparticles-Decorated Carbon Nanotube using Laser Ablation in Liquid and their Antimicrobial Activity. *Artificial cells, nanomedicine, and biotechnology*, **45**(8):1699-1709.
4. Khashan, K. S., Jabir, M. S. and Abdulameer, F. A. **2018**. Preparation and characterization of copper oxide nanoparticles decorated carbon nanoparticles using laser ablation in liquid. *Journal of Physics: Conference Series*, **1003**(1):012100.
5. Khashan, K. S. and Mahdi, M. **2017**. Preparation of indium-doped zinc oxide nanoparticles by pulsed laser ablation in liquid technique and their characterization. *Applied Nanoscience*, **7**(8): 589-596
6. Khashan, K. S. and Mahdi, F. **2017**. Synthesis of ZnO: Mg nanocomposite by pulsed laser ablation in liquid. *Surface Review and Letters*, **24**(7): 1750101.
7. Khashan, K.S., Sulaiman, G. M., Hamad, A., Abdulameer, F. A. and Hadi, A. **2017**. Generation of NiO nanoparticles via pulsed laser ablation in deionised water and their antibacterial activity. *Appl. Phys. A*, **123**: 190
8. Ismail, R. A., khashan, K.S. and Mahdi, R. O. **2017**. Characterization of high photosensitivity nanostructured 4H-SiC/p-Si heterostructure prepared by laser ablation of silicon in ethanol. *Materials Science in Semiconductor Processing*, **68**: 252-261
9. Krstulović, N., Salamon, K., Budimlija, O., Kovač, J., Dasović, J., Umek, P. and Capan, I. **2018**. Parameters optimization for synthesis of Al-doped ZnO nanoparticles by laser ablation in water. *Applied Surface Science*, **440**: 916-925.
10. Hameed, R., Khashan, K. S. and Sulaiman, G. M. **2020**. Preparation and characterization of graphene sheet prepared by laser ablation in liquid. *Materials today proceedings*, **20**: 535-539
11. Khashan, K. S., Taha, J. M. and Abbas, S. F. **2017**. Fabrication and Properties of InN NPs/Si as a photodetector . *Energy Procedia*, **119**: 656-661
12. Ismail, R.A., Khashan, K. S., Jawad, M. F., Mousa, A. M. and Mahdi, F. **2018**. Preparation of low cost n-ZnO/MgO/p-Si heterojunction photodetector by laser ablation in liquid and spray pyrolysis. *Materials Research Express*, **5**: 055018
13. ganesh, R. S., Navaneethan, M., Mani, G. K., Ponnusamy, S., Tsuchiya, K., Muthamizhchelvan, C., Kawasaki, S. and Hayakawa, Y. **2017**. Influence of Al doping on the structural, morphological, optical, and gas sensing properties of ZnO nanorods. *Journal of Alloys and Compounds*, **698** : 555-564.
14. Duque, J.S., Madrigal, B.M., Riascos, H., and Avila, Y.P. **2019**. Colloidal Metal Oxide Nanoparticles Prepared by Laser Ablation Technique and Their Antibacterial Test. *Colloids and Interfaces*, **3**: 25.
15. Khashan, K. S., Hassan, A. I., and Addie, A. J. **2016**. Characterization of CuO thin films deposition on porous silicon by spray pyrolysis. *Surface Review and Letters*, **23**:1650044
16. Khashan, K. S., Sulaiman, G. M., Abdulameer, F. A., and Napolitano, G. **2016**. Synthesis, characterization and antibacterial activity of colloidal NiO nanoparticles. *Pak. J. Pharm. Sci*, **29**: 541-546
17. Ismail, R. A., Mousa, A. M., Khashan, K. S., Mohsin, M. H., and Hamid, M. K. **2016**. Synthesis of PbI<sub>2</sub> nanoparticles by laser ablation in methanol. *Journal of Materials Science: Materials in Electronics*, **27**: 10696-10700
18. Khashan, K. S. **2011**. Optoelectronic properties of ZnO nanoparticles deposition on porous silicon. *International Journal of Modern Physics B*, **25**: 277–282
19. Bhatia, S., Verma, N. and Bedi, R. K. **2017**. Ethanol gas sensor based upon ZnO nanoparticles prepared by different techniques. *Results in physics*, **7**: 801-806.

20. Ezealisiji, K.M., Siwe-Noundou, X., Maduelosi, B., Nwachukwu, N. and Maçedo rause, R. W. 2019. Green synthesis of zinc oxide nanoparticles using *Solanum torvum* (L) leaf extract and evaluation of the toxicological profile of the ZnO nanoparticles–hydrogel composite in Wistar albino rats. *International Nano Letters*, **9**: 99-107
21. Khudair D. Y. and Al Ansari R. A. 2020. Impact of ZnO Atomic Ratio on Structural, Morphological and Some Optical Properties of  $(\text{SnO}_2)_{1-x}(\text{ZnO})_x$  Thin Films. *Iraqi Journal of Science*, **61**(2): 333-340.
22. Mustafa S. K., Jamal R. K. and AadimK. A. 2019. Studying the Effect of Annealing on Optical and Structure Properties of ZnO Nanostructure Prepared by Laser Induced Plasma. *Iraqi Journal of Science*, **60**(10): 2168-2176.
23. Davoud, D., Solati, E. and Dejam, L. 2012. Photoluminescence of ZnO nanoparticles generated by laser ablation in deionized water. *Applied Physics A*, **109**: 307-314
24. Raut, S., Thorat, P.V.D. and Thakre, R. 2015. Green synthesis of zinc oxide (ZnO) nanoparticles using *Ocimum tenuiflorum* leaves. *International Journal of Science and Research*, **4**: 1225-1228.
25. Zhang, P., Hong, R.Y., Chen, Q., Feng, W.G., and Badami, D. 2014. Aluminum-doped zinc oxide powders: synthesis, properties and application. *J Mater Sci: Mater Electron*, **25**:678–692
26. Bhuiyan, M. R. A., Alam, M. M., Momin, M. A. and Mamur, H. 2017. Characterization of Al doped ZnO nanostructures via an electrochemical route. *International Journal of Energy Applications and Technologies*, **4**: 28-33
27. Kumar, S. S., Venkateswarl, P., Rao, V. R. and Rao, G. N. 2013. Synthesis, characterization and optical properties of zinc oxide nanoparticles. *International Nano Letters*, **3**: 30.
28. Moazzen, M. A. M., Borghei, S. M. and Taleshi, F. 2013. Change in the morphology of ZnO nanoparticles upon changing the reactant concentration. *Appl Nanosci*, **3**: 295–302
29. Alkahlout, A., AlDahoudi, N., Grobelsek, I., Jilavi, M. and de Oliveira, P. W. 2014. Synthesis and Characterization of Aluminum Doped Zinc Oxide Nanostructures via Hydrothermal Route. *Journal of Materials*, **2014**: 1-8
30. Aimable, A., Strachowski, T., Wolska, E., Lojkowski, W. P. and Bowen, P. 2010. Comparison of two innovative precipitation systems for ZnO and Al-doped ZnO nanoparticle synthesis. *Processing and Application of Ceramics*, **4**: 107–114
31. Manoharan, C., Pavithra, G., Bououdina, M., Dhanapandian, S. and Dhamodharan, P. 2016. Characterization and study of antibacterial activity of spray pyrolysed ZnO:Al thin films. *Applied Nanoscience*, **6**: 815–825
32. Thandavan, T. M. K., Gani, S. M. A., San, W. C. M. d. and Nor, R. 2015. Enhanced Photoluminescence and Raman Properties of Al-Doped ZnO Nanostructures Prepared Using Thermal Chemical Vapor Deposition of Methanol Assisted with Heated Brass. *PLoS ONE*, **10**(3): e0121756. doi:10.1371/journal.pone.0121756